JOC Article

Structure−Function Studies of Modular Aromatics That Form Molecular Organogels

Christopher Baddeley, Zhiqing Yan, Graham King, Patrick M. Woodward, and Jovica D. Badjić*

Department of Chemistry, The Ohio State University, 100 West 18th Avenue, Columbus, Ohio 43210

badjic@chemistry.ohio-state.edu

Received June 1, 2007

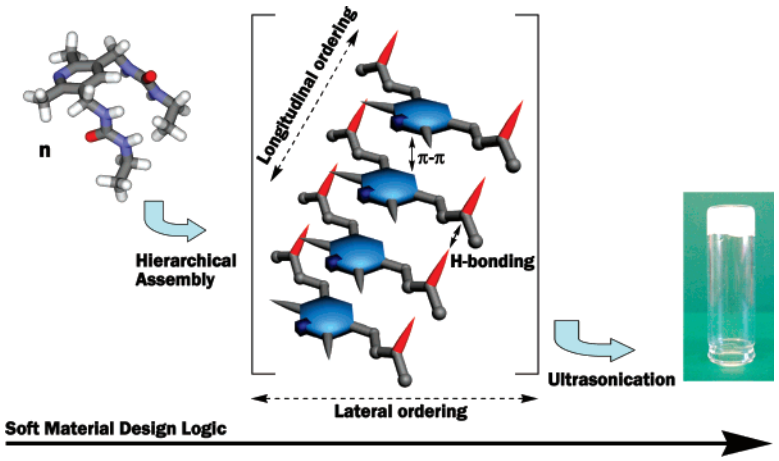

Three urea-based aromatics **1**−**3**, each with distinct steric and electronic characteristics, have been synthesized and their ability to undergo hierarchical assembly and gel organic solvents investigated. We have found that compound **1** promotes the sol−gel phase transition in primary alcohols (from CH_3OH to $C_{10}H_{21}OH$; CGC < 15 mg/mL), while **2** and **3** do not. IR spectroscopy, X-ray powder diffraction (XRPD), and transmission electron microscopy (TEM) measurements show that **1** organizes into "cylinders" in primary alcohols, using three-centered hydrogen bonds and $\pi-\pi$ aromatic interactions. The cylinders further organize into pairs through interdigitation of the methyl groups of the adjacent aromatic rings. Importantly, the lateral packing of the cylinders is enhanced as the bulk solvent polarity increases providing a mechanism for controlling the material's morphology via the solvophobic effect. Molecular mechanics (Amber) and semiempirical (AM1) calculations suggested similar conformational behavior but distinct electronic properties of **1**−**3**. Thus, π-deficient **2** without the methyl groups and π-rich **3** without aromatic nitrogen fail to promote the sol−gel phase transition in alcohols due to their inability to undergo effective hierarchical assembly, which is necessary for the formation of a 3D fibrillar network. In addition, we have found that the ultrasonication of a supersaturated solution of **1** is necessary for the gelation. Presumably, a fast exchange of the aggregates of **1** is assisted with sonic waves to allow for the effective and "error free" assembly wherein an entangled net of fibers capable of encapsulating solvent molecules is formed.

Introduction

Nowadays, there exists a strong technological and scientific drive to develop predictive tools for the rational design of low molecular weigh compounds (LMWGs) that can gel organic solvents.[1] The relationships between the structure of such molecules, their propensity to organize into self-assembled fibrillar networks (SAFINs), and the rheological (and other useful) properties of these gels are not fully developed.[2] The fundamental structure−function studies,[3] following the prin-

* Address correspondence to this author. Phone: (614) 247-8342. Fax: (614) 292-1685.

10.1021/jo071159y CCC: $37.00
Published on Web 08/23/2007

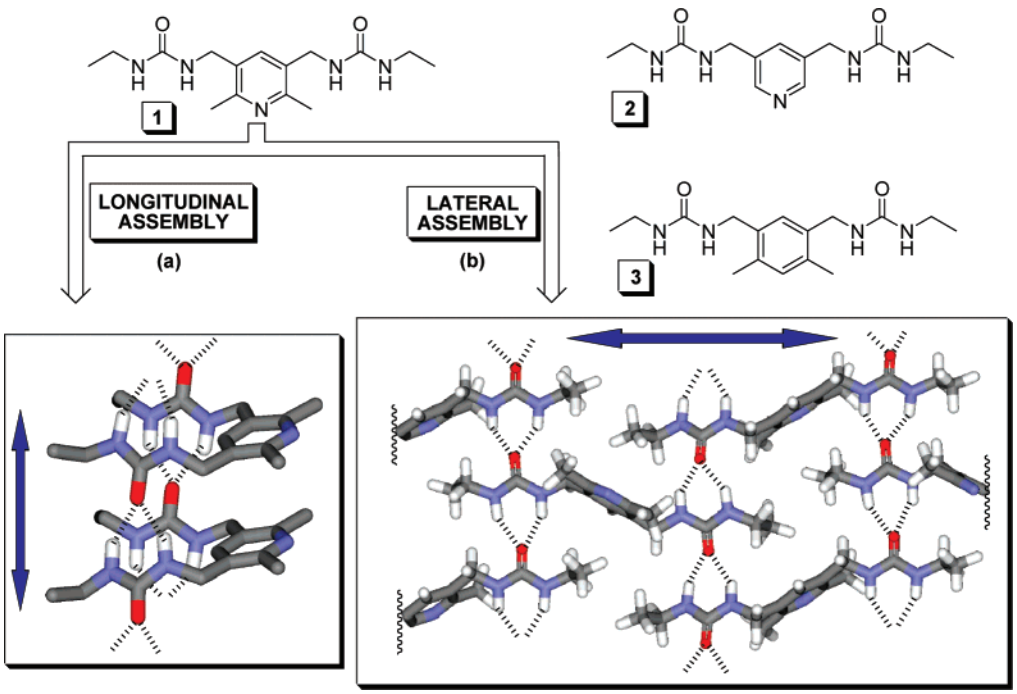

FIGURE 1. Chemical structures of **1**−**3**, and energy minimized (molecular mechanics, MM2) longitudinal (a) and lateral (b) assembly of **1**.

ciples of self-assembly and molecular engineering,[4] can transform the contemporary design of organogels from a somewhat serendipitous approach to a more rational one. In that vein, the study presented herein addresses both the structural and electronic requirements needed for small functional compounds to effectively assemble[5] and trigger the microscopic phase separation needed to gel organic solvents, including the role of solvent in such processes.[6]

Flory, early on,[7] referred to gels as materials with continuous structure and macroscopic appearance persistent on the time scale of our day-to-day activities, which are viscoelastic and solid-like below a certain stress limit. For the physical organogels of interest in this study, LMWGs are known to assemble into fibrillar 3D networks that in supersaturated solutions (sols) cause a phase transition to macroscopically immobilize the solvent molecules via surface tension and capillary forces.[1b] Such solid-like materials (gels) are composed largely of the liquid phase (typically ≥98%) and a rather small quantity of the *gelator*.

It has been recognized that anisotropic intermolecular interactions are a prerequisite for enhancing the linear aggregation of LMWGs while attenuating the growth along other dimensions, which allows for the gel formation.[8] On the basis of this principle, we have designed a series of divalent urea-based aromatics (Figure 1), all capable of interacting via hydrogen bonding, and examined their propensity to gel organic solvents. These molecules were chosen so as to explore the impact of systematic structural and electronic perturbations on their propensity to organize and form gels. Intriguingly, we discovered that a delicate balance between both the molecular structure

(1) (a) DeRossi, D.; Kajiwara, K.; Osada, Y.; Yamauchi, A., Eds. *Polymer Gels. Fundamentals and Biomedical Applications*; Plenum: New York, 1991. (b) Terech, P.; Weiss, R. G. *Chem. Rev.* **1997**, *97*, 3133. (c) Osada, Y.; Khokhlov, A. R., Eds. *Polymer Gels and Networks*; Marcel Dekker Inc.: New York, 2002. (d) Mallia, V. A.; Tamaoki, N. *Chem. Soc. Rev.* **2004**, *33*, 76. (e) Jung, J. H.; Shinkai, S. *Top. Curr. Chem.* **2005**, *248*, 223. (f) Carretti, E.; Dei, L.; Weiss, R. G. *Soft Matter* **2005**, *1*, 17−22. (g) Wang, R-Y.; Liu, X-Y.; Narayanan, J.; Xiong, J-Y.; Li, J-L. *J. Phys. Chem. B* **2006**, *110*, 25797. (h) Weiss, R. G.; Terech P., Eds. *Molecular Gels*: *Materials with Self-Assembled Fibrillar Networks*; Springer: Dordrecht, The Netherlands, 2006.

(2) (a) Van, E. J. H.; Feringa, B. L. *Angew. Chem., Int. Ed.* **2000**, *39*, 2263. (b) Suzuki, M.; Nakajima, Y.; Yumoto, M.; Kimura, M.; Shirai, H.; Hanabusa, K. *Org. Biomol. Chem.* **2004**, *2*, 1155. (c) Estroff, L. A.; Hamilton, A. D. *Chem. Rev.* **2004**, *104*, 1201. (d) de Loos, M.; Feringa, B. L.; van Esch, J. H. *Eur. J. Org. Chem.* **2005**, *17*, 3615. (e) Sangeetha, N. M.; Maitra, U. *Chem. Soc. Rev.* **2005**, *34*, 821. (f) Hirst, A. R.; Smith, D. K.; Harrington, J. P. *Chem. Eur. J.* **2005**, *11*, 6552. (g) Li, J. L.; Liu, X. Y.; Strom, C. S.; Ying, X. J. *Adv. Mat.* **2006**, *18*, 2574. (h) Escuder, B.; LLusar, M.; Miravet, J. F. *J. Org. Chem.* **2006**, *71*, 7747. (i) George, M.; Weiss, R. G. *Acc. Chem. Res.* **2006**, *39*, 489. (j) Ballabh, A.; Trivedi, D. R.; Dastidar, P. *Chem. Mater.* **2006**, *18*, 3795. (k) Weng, W.; Beck, J. B.; Jamieson, A. M.; Rowan, S. J. *J. Am. Chem. Soc.* **2006**, *128*, 11663. (l) Rieth, S.; Baddeley, C.; Badjić, J. D. *Soft Matter* **2007**, *1*, 137.

(3) (a) Mieden-Gundert, G.; Klein, L.; Fischer, M.; Vogtle, F.; Heuze, K.; Pozzo, J-L.; Vallier, M.; Fages, F. *Angew. Chem., Int. Ed.* **2001**, *40*, 3164. (b) Malik, S.; Maji, S. K.; Banerjee, A.; Nandi, A. K. *J. Chem. Soc., Perkin Trans. 2* **2002**, *6*, 1177. (c) Potluri, V. K.; Hamilton, A. D. *J. Supramol. Chem.* **2003**, *2*, 321. (d) Ishi-i, T.; Shinkai, S. *Top. Curr. Chem.* **2005**, *258*, 119. (e) Serpe, M. J.; Craig, S. L. *Langmuir* **2007**, *23*, 1626.

(4) (a) Philp, D.; Stoddart, J. F. *Angew. Chem., Int. Ed. Engl.* **1996**, *35*, 1155. (b) Whitesides, G. M.; Grzybowski, B. *Science* **2002**, *295*, 2418. (c) Ikkala, O.; ten Brinke, G. *Chem. Commun.* **2004**, *19*, 2131. (d) Lehn, J-M. In *Supramolecular Polymers*; Ciferri, A., Ed.; CRC Press LLC: Boca Raton, FL, 2005; p 3. (e) Fialkowski, M.; Bishop, K. J. M.; Klajn, R.; Smoukov, S. K.; Campbell, C. J.; Grzybowski, B. A. *J. Phys. Chem. B* **2006**, *110*, 2482.

(5) (a) Hanabusa, K.; Yamada, M.; Kimura, M.; Shirai, H. *Angew. Chem., Int. Ed. Engl.* **1996**, *35*, 1949. (b) van Esch, J.; Kellogg, R. M.; Feringa, B. L. *Tetrahedron Lett.* **1997**, *38*, 281. (c) Schoonbeek, F. S.; Van Esch, J. H.; Wegewijs, B.; Rep, D. B. A.; De Haas, M. P.; Klapwijk, T. M.; Kellogg, R. M.; Feringa, B. L. *Angew. Chem., Int. Ed.* **1999**, *38*, 1393. (d) George, M.; Snyder, S. L.; Terech, P.; Glinka, C. J.; Weiss, R. G. *J. Am. Chem. Soc.* **2003**, *125*, 10275. (e) Liu, Y.; Li, Y.; Jiang, L.; Gan, H.; Liu, H.; Li, Y.; Zhuang, J.; Lu, F.; Zhu, D. *J. Org. Chem.* **2004**, *69*, 9049. (f) Nie, X.; Wang, G. *J. Org. Chem.* **2006**, *71*, 4734. (g) Chow, H-F.; Zhang, J.; Lo, C-M.; Cheung, S-Y.; Wong, K-W. *Tetrahedron* **2006**, *63*, 363.

(6) (a) Zhu, G.; Dordick, J. S. *Chem. Mater.* **2006**, *18*, 5988. (b) Pinault, T.; Isare, B.; Bouteiller, L. *ChemPhysChem* **2006**, *7*, 816.

(7) (a) Flory, P. J. *J. Phys. Chem.* **1942**, *46*, 132. (b) Flory, P. J. *Faraday Discuss. Chem. Soc.* **1974**, *57*, 7.

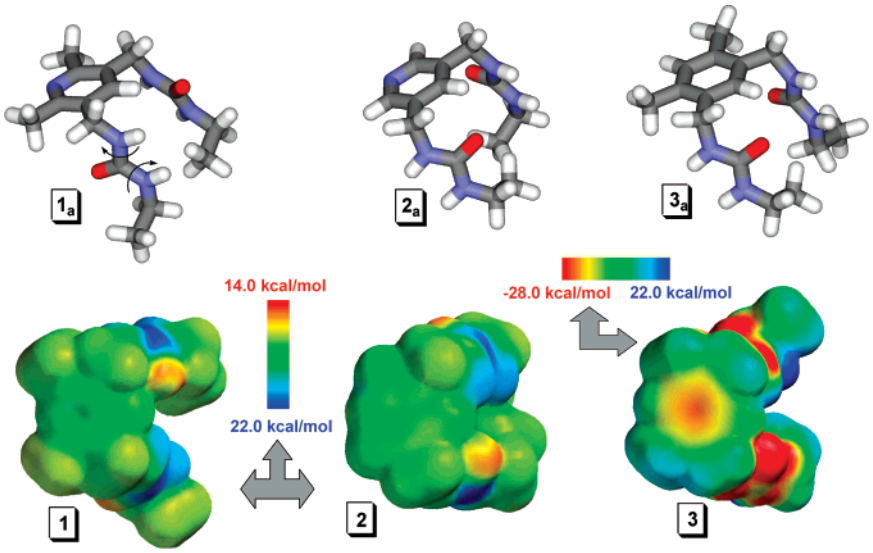

FIGURE 2. (A) Calculated global minimum energy conformers of **1**−**3**, obtained with Monte Carlo conformational search (Amber*). (B) Electrostatic potential surface maps of energy minimized $\mathbf{1_a}$−$\mathbf{3_a}$ (AM1, Spartan Software).

and electronic properties of our LMWGs, as well as the solvent polarity, is important to achieve gelation and control the morphology of the assembled fibers. We also revealed that ultrasonication of supersaturated solutions is necessary to complete the sol−gel transition with our gelators.

Results and Discussion

Design Logic, Hypothesis, and Motivation. It has long been known that molecules carrying urea functionality(ies) organize into hydrogen-bonded networks.[9] *Intermolecular* three-center hydrogen bonds, encoded as $R_2^1(\mathbf{6})$,[10] are usually formed between the carbonyl group of one urea molecule and the N−H groups of the adjacent one. *N*,*N*′-Disubstituted ureas have thus been shown to associate into oligomeric one-dimensional chains in both solution and the solid state.[11] Bouteiller et al. have, in particular, studied the morphology and cooperativity for the assembly of low molecular weight bis-ureas forming organogels in nonpolar solvents.[11b−d] Typically observed formation of short chains in solution results from a weak interaction between the repeating monovalent units. Therefore, increasing the number of urea functionalities within a single unit[5] augments the avidity of the multivalent monomers for assembly on account of the multivalency effect[12]—the entropic gain is attained through the multiplication of monovalent into multivalent units. With that in mind we designed compounds **1**−**3**, each containing two urea functionalities bridged with an aromatic linker, to create a situation in which a strong anisotropic ordering can take place (Figure 1).

The *longitudinal* assembly (Figure 1a) portrays the urea functional units in **1**−**3** stacked on top of one another, directing the chain propagation orthogonally to the plane of the aromatic scaffolds. In contrast, the *lateral* assembly (Figure 1b) incorporates the self-complementary ureas organizing into a two-dimensional plane, with a molecule linking four neighboring molecules together so that the hydrogen-bonding sites are entirely exploited. This arrangement disqualifies the aromatic stacking and is entropically more expensive. In that regard, the morphology of the supramolecular array is expected to favor the *longitudinal* arrangement. Even so, the nature of the surrounding solvent and the scaffold holding the urea functionalities can play a determining role for the assembly thermodynamics and mechanism.

Compounds **1**−**3** incorporate rigid aromatic scaffolds, each with different steric and electronic properties (Figure 2). Molecular mechanics calculations have, in the past, been shown to be important for examining the assembly preference in medium-sized systems.[13] In the case of **1**−**3**, it indeed affords insight into the assembly pattern (Figure 1). However, hardly any information is available to develop a sound relationship between the compounds with slightly different molecular structures (**1**−**3**) and their genuine propensity for ordering and thereby triggering the sol-to-gel phase transition in liquids. What are the actual electronic and structural requirements for a molecule to assemble and gel organic solvents? Supposedly, the modular architectures of **1**−**3** (Figure 1) will allow us to explore this relationship. In continuation, the principles of

(8) (a) van Esch, J.; De Feyter, S.; Kellogg, R. M.; De Schryver, F.; Feringa, B. L. *Chem. Eur. J.* **1997**, *3*, 1238. (b) Van Esch, J.; Schoonbeek, F.; De Loos, M.; Kooijman, H.; Spek, A. L.; Kellogg, R. M.; Feringa, B. L. *Chem. Eur. J.* **1999**, *5*, 937. (c) De Loos, M.; Ligtenbarg, A. G. J.; Van Esch, J.; Kooijman, H.; Spek, A. L.; Hage, R.; Kellogg, R. M.; Feringa, B. L. *Eur. J. Org. Chem.* **2000**, *22*, 3675−3678. (d) Gronwald, O.; Shinkai, S. *Chem. Eur. J.* **2001**, *7*, 4328. (e) Mizoshita, N.; Monobe, H.; Inoue, M.; Ukon, M.; Watanabe, T.; Shimizu, Y.; Hanabusa, K.; Kato, T. *Chem. Commun.* **2002**, *5*, 428. (f) George, M.; Tan, G.; John, V. T.; Weiss, R. G. *Chem. Eur. J.* **2005**, *11*, 3243. (g) Hoeben, F. J. M.; Jonkheijm, P.; Meijer, E. W.; Schenning, A. P. H. J. *Chem. Rev.* **2005**, *105*, 1491.

(9) (a) Etter, M. C.; Urbanczyk-Lipkowska, Z.; Zia-Ebrahimi, M.; Panunto, T. W. *J. Am. Chem. Soc.* **1990**, *112*, 8415. (b) Masunov, A.; Dannenberg, J. J. *J. Phys. Chem. B* **2000**, *104*, 806. (c) Shimizu, L. S.; Hughes, A. D.; Smith, M. D.; Davis, M. J.; Zhang, B. P.; Zur Loye, H-C.; Shimizu, K. D. *J. Am. Chem. Soc.* **2003**, *125*, 14972. (d) Laliberte, D.; Maris, T.; Wuest, J. D. *Can. J. Chem.* **2004**, *82*, 386.

(10) Etter, M. C. *Acc. Chem. Res.* **1990**, *23*, 120.

(11) (a) Jadzyn, J.; Stockhausen, M.; Zywucki, B. *J. Phys. Chem.* **1987**, *91*, 754. (b) Lortie, F.; Boileau, S.; Bouteiller, L. *Chem. Eur. J.* **2003**, *9*, 3008. (c) Simić, V.; Bouteiller, L.; Jalabert, M. *J. Am. Chem. Soc.* **2003**, *125*, 13148. (d) Bouteiller, L.; Colombani, O.; Lortie, F.; Terech, P. *J. Am. Chem. Soc.* **2005**, *127*, 8893.

(12) Badjić, J. D.; Nelson, A.; Cantrill, S, J.; Turnbull, W. B.; Stoddart, J. F. *Acc. Chem. Res.* **2005**, *38*, 723.

(13) (a) Xia, T. K.; Landman, U. *Science* **1993**, *261*, 1310. (b) Song, J.; Hollingsworth, R. I. *J. Am. Chem. Soc.* **1999**, *121*, 1851. (c) Xie, Z. X.; Xu, X.; Tang, J.; Mao, B. W. *Chem. Phys. Lett.* **2000**, *323*, 209.

SCHEME 1. Synthesis of Compounds 1−3

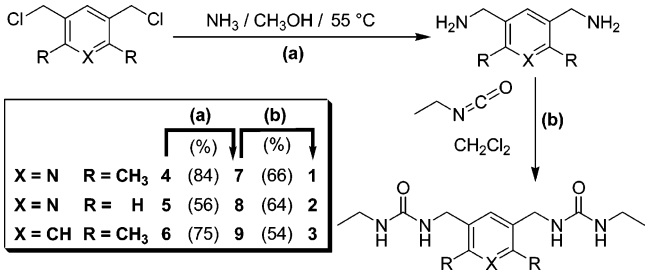

template-directed organic synthesis can be applied to engineer nanoscale structures, comprising **1**−**3** or related compounds, with intriguing macroscopic properties.

Synthesis. The preparation of **1**−**3** is outlined in Scheme 1. In a nucleophilic displacement reaction, (bis)chloromethyl aryl aromatics **4**−**6** were each reacted with ammonia to give diamines **7**−**9**. Compounds **4**−**6** were prepared in accord with already described literature procedures.[14] Following, the condensation of diamines **7**−**9** with ethylisocyanate gave rise to desired divalent ureas **1**−**3** in satisfactory high yields (Scheme 1).

Gelation Studies. At room temperature, compounds **1** and **3** were sparingly soluble in almost any solvent that we tried (<7 mg/mL). Compound **2**, however, showed better solubility behavior, particularly in polar alcoholic solvents (>70 mg/mL). Upon heating an alcoholic solution of **1** (Table 1), the compound gradually dissolved and at elevated temperatures (typically at the solvent boiling point) became completely solubilized. Interestingly, the subsequent cooling of such prepared solution did not lead to the gelation, unless sonication was applied (Figure 3).[15] The ultrasound evidently assists the microphase separation and formation of a 3D-network, which is necessary for solvent encapsulation. In fact, without ultrasonication, flocculation, and in some instances precipitation, of **1** was observed. The collapse of cavitation bubbles created by the ultrasound can be hypothesized to produce shear forces that mediate a more effective entanglement of the aggregates of **1**, thus partitioning the solvent molecules. Sound waves, on the other hand, have been known to stimulate rapid translational and rotational molecular movements which shorten the lifetime of noncovalent complexes and promote the disruption of aggregates.[16] Consequently, the observed ultrasound-promoted phase transition can be qualitatively rationalized by presuming that the lifetime of the aggregates of **1** is indeed a function of the ultrasound, under the experimental conditions. Accordingly, a statistically distributed mixture of aggregates of **1** in the supersaturated solution (sol) undergoes a more facile interconversion of the ensemble members when aided by ultrasonication. The ultrasound-promoted combinatorial exchange of the thermodynamic states in the system[17] thus "proofreads" the aggregation, eliminates possible "errors", and allows for the effective gelation. In the absence of the ultrasonication the exchange became slow, leading to the "kinetic" aggregation that results in precipitation or flocculation.

TABLE 1. Minimum Amount of Compound 1 (CGC) Necessary for Gelation (Compounds 2 and 3 Were Incapable of Hardening the Alcoholic Solvents) and Dimroth−Reichardt $E_T(30)$ Solvent Polarity Parameters[38]

solvent	CGC (g/L)	$E_T(30)$
methanol	15	55.4
ethanol	12	51.9
n-propanol	8	50.7
isopropanol	N/G	48.4
n-butanol	6	49.7
tert-butanol	N/G	43.3
n-pentanol	5	49.1
n-hexanol	6	48.8
cyclohexanol	N/G	47.2
n-heptanol	6	48.5
n-octanol	6	48.1
isooctanol	N/G	
n-decanol	6	47.7

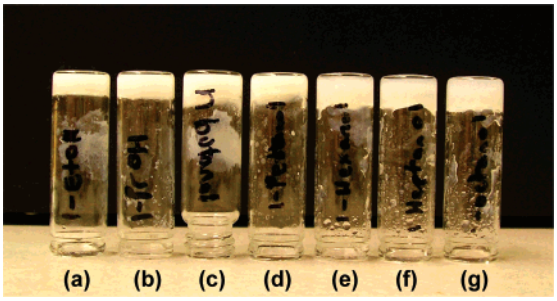

FIGURE 3. Photograph showing inverted vials with each containing the gel phase of compound **1** formed in (a) ethanol, (b) 1-propanol, (c) 1-butanol, (d) 1-pentanol, (e) 1-hexanol, (f) 1-heptanol, and (g) 1-octanol. The gels have been shown to be persistent, without changing appearance for at least 6 months at ambient temperature.

Compounds **2** and **3** would not harden any of the examined alcohols (Table 1), regardless of the procedure or their initial concentration. Notably, the electronic and structural information incorporated in these two molecules, subtly different from that in **1**, mirrored into considerably different behavior at the macroscopic scale!

A careful inspection of Table 1 shows that only primary alcohols are gelated with **1**, suggesting a possible role of the solvent molecules in the assembly.[6] As **1** incorporates a pyridine ring, the molecules of primary alcohols can be expected to hydrogen bond to it by sharing their proton with the pyridine nitrogen. With that in mind, branching a linear chain in the alcohol can introduce the van der Waals strain in the assembly that upsets the packing, lowers the stability, and deters the formation of aggregates. It is also evident from Table 1 that compound **1** gels alcoholic solvents of different polarity.

Infrared Spectroscopy (IR): Hydrogen Bonding-Driven Assembly. The premise of our work was based on the prior understanding of the aggregation behavior of ureas and their ability to form three-centered hydrogen bonds. Verifying the

(14) (a) Tsuda, K.; Ikekawa, N.; Mishima, H.; Ilino, A.; Morishage, T. *Pharm. Bull. Jpn.* **1953**, *1*, 122. (b) Mathia, J.; Seto, C.; Simanek, E.; Whitesides, G. M. *J. Am. Chem. Soc.* **1994**, *116*, 1725. (c) Starnes, S. D.; Rudkevich, D. M.; Rebek, J., Jr. *J. Am. Chem. Soc.* **2001**, *123*, 4659. (d) Collman, J. P.; Decreau, R. A.; Constanzo, S. *Org. Lett.* **2004**, *6*, 1033. (e) Tsuge, A.; Matsubara, A.; Moriguchi, T. *Tetrahedron Lett.* **2006**, *37*, 6607.

(15) For an example of the ultrasound promoted sol−gel phase transition, see: Naota, T.; Koori, H. *J. Am. Chem. Soc.* **2005**, *127*, 9324.

(16) (a) Paulusse, J. M. J.; Sijbesma, R. P. *Angew. Chem., Int. Ed.* **2006**, *45*, 2334. (b) Paulusse, J. M. J.; Huijbers, J. P. J.; Sijbesma, R. P. *Chem. Eur. J.* **2006**, *12*, 4928.

(17) The concept of dynamic combinatorial chemistry is based on the fast exchange of various host−guest thermodynamic states. See: (a) Rowan, S. J.; Cantrill, S. J.; Cousins, G. R. L.; Sanders, J. K. M.; Stoddart, J. F. *Angew. Chem., Int. Ed.* **2002**, *41*, 899. (b) Corbett, P. T.; Leclaire, J.; Vial, L.; West, K. R.; Wietor, J-L.; Sanders, J. K. M.; Otto, S. *Chem. Rev.* **2006**, *106*, 3652.

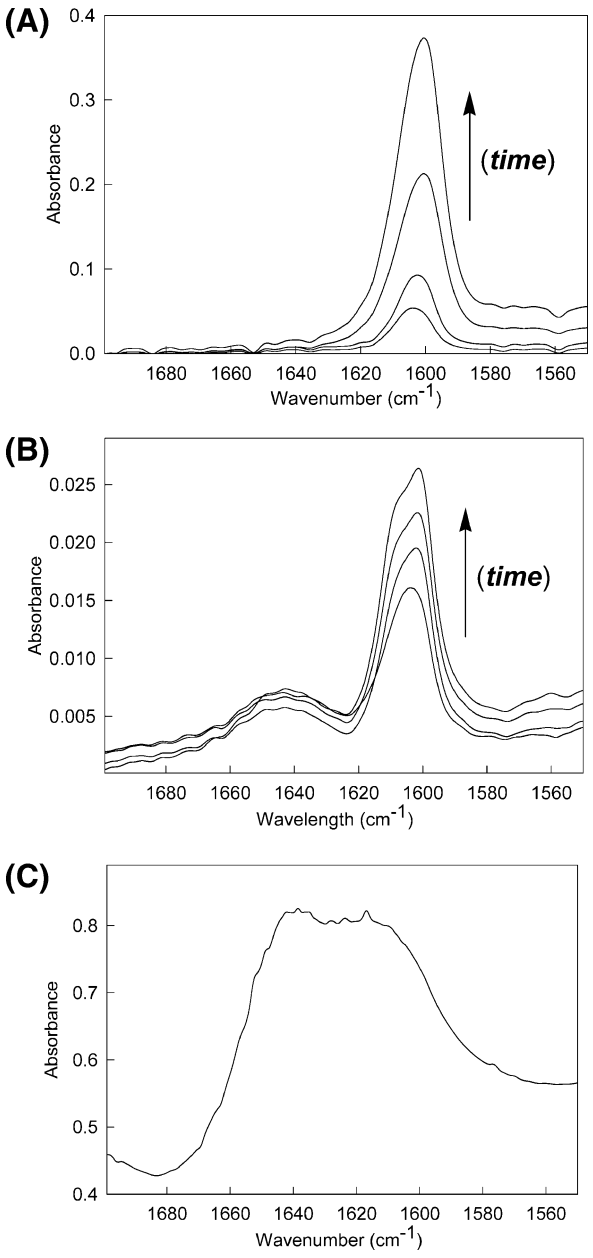

FIGURE 4. C═O stretch region of infrared spectra of **1** obtained from (A) a thin film of its gel sample (18.0 mM, CD_3OD) deposited on the transmitting crystal (ATR-IR) and acquired after 0, 5, 15, and 40 min, at ambient temperature, (B) a 18.0 mM supersaturated solution of **1** (CD_3OD) at 70 °C deposited on the transmitting cryatel (ATR-IR) and acquired after 1, 4, 6, and 12 min at room temperature, and (C) a 7.0 mM CD_3OD solution of **1** (below CGC), contained in a long path, 10 mm, liquid cell.

existence of N−H−O═C noncovalent interactions, in addition to the prospect of obtaining a mechanistic insight into the assembly of **1**, prompted systematic and thorough IR spectroscopic studies of the gelation. We, therefore, conducted a detailed FT-IR study (attenuated total reflectance method) of a gel sample of **1** in CD_3OD (Figure 4A). Also, we obtained IR spectra of a supersaturated solution of **1** in CD_3OD, with real-time FT-IR "snapshots" of the gelation process (Figure 4B). In addition, a CD_3OD solution **1** below the compound's critical gelation concentration (CGC) was examined (Figure 4C). The FT-IR spectrum of the gel (Figure 4A) revealed a strong and rather sharp C═O stretching band at 1604 cm^{-1}. As the solvent (CD_3OD) evaporated over time (40 min), the position of the band remained unchanged. The FT-IR spectrum of a hot supersaturated CD_3OD solution of **1** (Figure 4B) revealed three major C═O stretching vibrations—a weak and broad vibration at 1645 cm^{-1}, a strong and sharp vibration at 1604 cm^{-1}, and a shoulder-like vibration at 1610 cm^{-1}. As the solution cooled and the flocculation occurred, the relative intensity of the sharper peak increased while the broad signal remained almost unaffected.

The xerogel formation (Figure 4A), caused by the solvent evaporation of the gel sample, had no apparent effect on the carbonyl stretch frequency, indicating a uniform environment for this functional group during the phase transition. This points to the absence of hydrogen bonding between the solvent molecules and the carbonyl oxygens in **1**, in the gel phase. That is to say, the urea moieties in **1** are likely to be themselves engaged in forming uniform hydrogen bonds in the gel, to give rise to the sharp carbonyl stretch at 1604 cm^{-1} (Figure 4A).

The analogous carbonyl vibration (1604 cm^{-1}) also developed with the maturation of the supersaturated solution of **1** (Figure 4B). Evidently, the aggregates $\mathbf{1}_{[n]}$ occurred before the microphase separation was even completed. Interestingly, this suggests the prospect of the spontaneous nucleation mechanism operating in the gelation.[18] A more detailed study is, however, necessary to provide information about the assembly mechanism. The ineffective gel formation, due to the absence of ultrasonication, is also noticeable (Figure 4B). Namely, the appearance of (a) a broad 1645 cm^{-1} signal likely corresponding to the carbonyl groups in **1** forming weak hydrogen bond(s) with CD_3OD molecules and (b) a shoulder-like vibration at 1610 cm^{-1} likely corresponding to the carbonyl group in **1** forming ill-defined and small aggregates, point to it. The broadness also implicates the existence of a fraction-weighted mixture of the conformers of **1** (Figure 2).

When the concentration of **1** was kept below the CGC (CD_3OD, 7.0 mM), the FT-IR analysis showed two broad bands centered at 1640 and 1610 cm^{-1}, respectively (Figure 4C). In accord with the prior discussion, the higher frequency stretch would correspond to the solvated, and the lower frequency stretch to the "imperfectly" aggregated molecules of **1**.

X-ray Powder Diffraction: Real Space Structure Solution. Since traditional structure determination techniques, such as single-crystal X-ray diffraction, do not lend themselves to organogels we have used X-ray powder diffraction (XRPD) to gain insight into the molecular packing of **1**. We obtained high-resolution XRPD patterns of the dried xerogel of **1** and applied real space structure solution methods to determine the molecular organization in the organogel. The strong well-resolved peaks observed in the XRPD pattern indicate that the molecular packing is well ordered. To extract structural information from the XRPD data, we first indexed the XRPD pattern to determine the crystal system and unit cell dimensions. Peak positions were obtained by analytically fitting the peak profiles. These positions served as the input for the autoindexing programs.[19] Autoindexing produced several possible unit cells with good figures of merit, all possessing triclinic symmetry. A total of five unique unit cells with distinct unit cell volumes were obtained. The

(18) Huang, X.; Terech, P.; Raghavan, S. R.; Weiss, R. G. *J. Am. Chem. Soc.* **2005**, *127*, 4336.

(19) Coelho, A. A. *Topas Academic*, General Profile and Structure Analysis Software for Powder Diffraction Data; Bruker AXS: Karlsruhe, Germany, 2004.

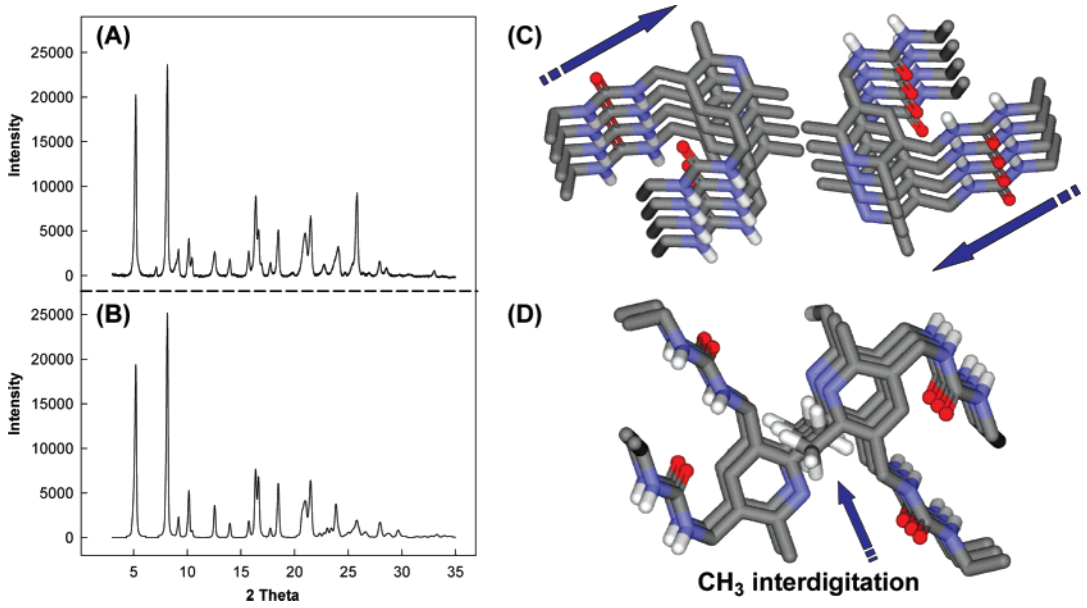

FIGURE 5. (A) High-resolution X-ray diffraction image of the xerogel of **1**. The material was obtained by drying a gel sample of **1** (22.0 mM, 1-butanol) at 80 °C for 1 h, and the data were collected from a thin film (1 mm) of the material deposited onto a glass substrate. (B) Computer-generated image of the X-ray diffraction spectrum of **1**, obtained via the algorithm of simulated annealing. (C and D) Ball and stick representations of the solid-state structure of **1** and its packing in the xerogel phase.

small peak at approximately 7.1° 2θ was excluded from the indexing process since all attempts to include it resulted in unreasonably large unit cells with poor figures of merit. This peak is thought to be due to the presence of a small impurity.

Next, real space structure solution was carried out for each unique unit cell that emerged from the autoindexing process. This structure solution process was performed by using a software[19−20] that utilizes a simulated annealing algorithm to find the location, orientation, and torsion angles of the molecule that give the best agreement between the experimental and calculated diffraction patterns. Space group $P\bar{1}$ was used in all cases and 30 runs per trail were performed. One unit cell provided a distinctly superior fit to the data. This unit cell was also the only one produced by both autoindexing programs independently. The dimensions of the unit cell were therefore determined to be a = 4.4570(11) Å, b = 11.0920(12) Å, c = 16.9610(19) Å, α = 95.67(1)°, β = 88.77(2)°, γ = 78.37(2)°, V = 815.78, Z = 2.

Initial simulated annealing runs consistently underestimated the intensity of the *hkl* peak located at 25.8° 2θ. This peak results from the overlap of two closely spaced peaks with *hkl* values of 0,−3,2 and 0,3,1. This raised the possibility that preferred orientation effects were present. Preferred orientation terms were introduced about the 0,−3,2, 0,3,1, and 0,1,0 axes, with the 0,−3,2 correction resulting in the greatest improvement to the fit. The value of the preferred orientation term was consistent with a needle-like crystal habit. This finding is supported by the TEM studies discussed in the next section. Since for chemical reasons the urea moiety is suspected of being nearly planar it was restricted to be so to help reduce the number of degrees of freedom.

The final structure solution is shown in Figure 5. The resulting crystal structure shows that the molecules adopt a longitudinal assembly (see Figure 1), as anticipated. The structure contains columns of pyridine rings stacked in a slipped mode with an antiparallel orientation. The distance between the rings is about 4.2 Å, which is slightly longer than is typical for optimal attractive $\pi-\pi$ interactions.[22] Apparently, steric interactions limit the close approach of the planar aromatic rings. The simulation is much less sensitive to the orientation of the urea moieties. Several otherwise similar solutions were obtained with similar figures of merit, but with different orientations of the urea group. Nevertheless, the solution suggests the possible formation of bifurcated hydrogen bonds orienting perpendicular to the planes or the aromatic rings. The simulation did prove sensitive to the angle between the pyridine ring and the linear chains with the connecting bond angle being approximately 53° relative to the plane of the pyridine ring.

A careful inspection of the ordering of **1** also revealed that the molecular columns further organize in pairs through interdigitation of the methyl groups of the adjacent aromatic rings (Figure 5D). This feature of the structure, which could not be anticipated a priori, denotes another level of the hierarchical organization. Consequently, the observed inability of **2** to gel organic solvents can, to a degree, be rationalized by the absence of the methyl group in its structure.

Due to the possibility of a phase transition and molecular transposition during the xerogel formation, the presented results need to be taken with some caution.[1g] We cannot exclude the possibility that the molecular assembly could undergo a reorganization during the preparation of a sample for X-ray studies. In particular, the results of the IR spectroscopic measurements (Figure 4A) suggest that such reorganization is not likely to occur.

Transmission Electron Microscopy (TEM). Transmission electron micrograph images of organogels of **1**, with different alcoholic solvents, display a web of entangled fibers (Figure

(20) David, W. I. F.; Shankland, K.; Shankland, N. *Chem. Commun.* **1998**, 931−932.

(21) David, W. I. F.; Shankland, K.; van de Streek, J.; Pidcock, E.; Motherwell, W. D. S.; Cole, J. C. *J. Appl. Crystallogr.* **2006**, *39*, 910−915.

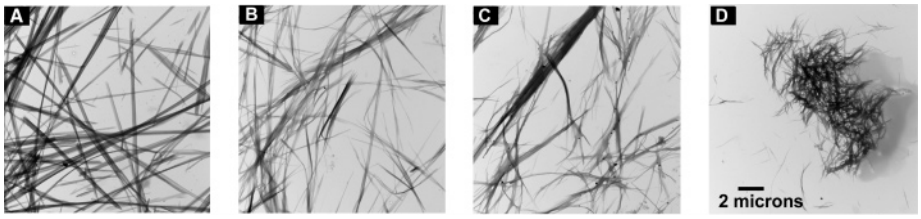

FIGURE 6. Electron microscope images (TEM) of dried gels of **1,** prepared in (A) 1-butanol, (B) 1-hexanol, (C) 1-heptanol, and (d) 1-decanol and deposited on a carbon coated Formvar grid. The diameter of the assembled fibers decreases in the series (from A to D), suggesting a role of the solvophobic effect in the hierarchical ordering.

6). The high aspect ratio of the fibers indicates highly anisotropic interactions between the gelator molecules, in agreement with a one-dimensional, hydrogen bonded, and $\pi-\pi$ stacked assembly of **1** (Figure 5). The fibers are several micrometers long, rod-like in *n*-butanol while intertwined and bundled in *n*-decanol (Figure 6A−D). Interestingly, the diameter of the fibers appears to be smaller in less polar *n*-decanol ($E_T(30) = 47.7$; the distribution is centered on 50 nm), than in more polar *n*-butanol ($E_T(30) = 49.7$; the distribution is centered on 700 nm). The thickness is related to the lateral ordering of the hydrogen-bonded columns of **1**, capable of developing van der Walls attractive interactions. These noncovalent forces, operating at the periphery of the assembled **1**, are weak and multiple, however, solvophobic in origin. As a result, changing the environmental polarity should have an effect on the free energy of the columnar assemblies, via the solvophobic effect.[23] Namely, a more polar solvent promotes the lateral column ordering and makes the fibers thicker (therefore long and straight). This hypothesis is indeed supported with the experimental results (Figure 6A−D).

Molecular Mechanics. Our molecular mechanics (MM2)[24] calculations of the energy minimized octomers of **1** suggested that two columns pack in the antiparallel orientation with respect to the aromatic nitrogens. The steric energy for such ordering is, interestingly, lower than that for other possible arrangements (see the Supporting Information for more details), which is in agreement with the refined xerogel structure of **1** (Figure 5).

Preorganization, Steric, and Electronic Effects. The effective assembly of LMWGs is important for the formation of a 3D molecular network that encapsulates solvent molecules and causes gel formation. Molecular recognition, in which functional molecules organize into ordered assemblies, requires molecular components to desolvate, conformationally preorganize, and interact using reversible noncovalent interactions.[25] As a result, the formation of molecular organogels may be conditioned with the level of preorganization[26] of the consisting molecular components, particularly if they sample rotational isomers within a narrow energy window.[27] Furthermore, the height of the energy barrier for the conversion of rotamers is fundamental for the conformational sampling, which in turn allows "error checking" and "proof reading" whereby a well-structured material is about to be formed. These details have prompted us to research the conformational and electronic behavior of *N*,*N*′-dialkyl ureas **1**−**3** (Figure 2).

SCHEME 2. Conformational Isomers of Symmetrical *N*,*N*′-Disubstituted Ureas, Created by Rotation about Their (O═)C−N Bonds

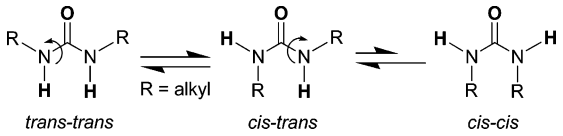

N,*N*′-Disubstituted ureas adopt three (or four) conformations with the rotation of the substituents about the (O═)C−N bonds (Scheme 2). Calculations at both low and high level of theory,[28] IR and NMR spectroscopic measurements,[29,30] and X-ray solid-state data[9,10] all indicate that symmetrical dialkylureas preferentially assume *trans*−*trans* and *cis*−*trans*, but not *cis*−*cis* conformations. The rotation about the (O═)C−N bond in ureas is hindered, which has been explained by delocalization of the nitrogen lone-electron pair into the carbonyl group to increase the (O═)C−N bond order.[31] Depending on the level of theory, the activation barrier for the rotation about the (O═)C−N bond in variously substituted ureas has been calculated to be in the range of 7−10 kcal/mol.[32] The experimentally determined barriers are below 11.5 kcal/mol, and also solvent dependent.[33]

With this in mind, we completed a conformational analysis of **1**−**3** using molecular mechanics (Amber)[33] and the Monte Carlo method for stochastic conformational sampling (Figure 2A). As implemented in MacroModel, the results of the calculated free energy differences suggested "*trans*" $\mathbf{1_a}$, $\mathbf{2_a}$, or $\mathbf{3_a}$ (Figure 2A) as the most favorable conformers for each series of compounds. The Boltzmann population distribution, however,

(22) (a) Hunter, C. A.; Lawson, K. R.; Perkins, J.; Urch, C. J. *J. Chem. Soc., Perkin Trans. 2* **2001**, *5*, 651. (b) Meyer, E. A.; Castellano, R. K.; Diederich, F. *Angew. Chem., Int. Ed.* **2003**, *42*, 1210.
(23) Feiters, M. C.; Nolte, R. J. M. *Adv. Supramol. Chem.* **2000**, *6*, 41.
(24) (a) Allinger, N. L. *J. Am. Chem. Soc.* **1977**, *99*, 8127. (b) Allinger, N. L.; Kok, R. A.; Imam, M. R. *J. Comput. Chem.* **1988**, *9*, 591.
(25) (a) Rebek, J. Jr. *Science* **1987**, 235, 1478. (b) Cram, D. J. *Science* **1988**, *240*, 760.
(26) Cram, D. J *Angew. Chem.* **1986**, *98*, 1041.
(27) Cannon, W. R.; Madura, J. D.; Thummel, R. P.; McCammon, J. A. *J. Am. Chem. Soc.* **1993**, *115*, 879.
(28) (a) Kontoyianni, M.; Bowen, J. P. *J. Comput. Chem.* **1992**, *13*, 657. (b) Galabov, B.; Ilieva, S.; Hadjieva, B.; Dudev, T. *J. Mol. Struct.* **1997**, *407*, 47−51. (c) Lecomte, F.; Lucas, B.; Gregoire, G.; Schermann, J. P.; Desfrancois, C. *Phys. Chem. Chem. Phys.* **2003**, *5*, 3120. (d) Custelcean, R.; Gorbunova, M. G.; Bonnesen, P. V. *Chem. Eur. J.* **2005**, *11*, 1459.
(29) (a) Rao, C. N. R.; Rao, K. G.; Goel, A.; Balasubramanian, D. *J. Chem. Soc. A* **1971**, *19*, 3077. (b) Mido, Y. *Spectrochim. Acta* **1973**, 29. (c) Mido, Y. *Bull. Chem. Soc. Jpn.* **1974**, *47*, 1833. (d) Mido, Y.; Gohda, T. *Bull. Chem. Soc. Jpn.* **1975**, *48*, 2704.
(30) (a) Filleux-Blanchard, M. L.; Durand, A. *Org. Magn. Reson.* **1971**, *3*, 187. (b) Olofsson, G.; Stilbs, P.; Drakenberg, T.; Forsen, S. *Tetrahedron* **1971**, *27*, 4583. (c) Hartman, J. S.; Schrobilgen, G. J. *Can. J. Chem.* **1973**, *51*, 99.
(31) Anet, F. A. L.; Ghiaci, M. *J. Am. Chem. Soc.* **1979**, *101*, 6857.
(32) (a) Haushalter, K. A.; Lau, J.; Roberts, J. D. *J. Am. Chem. Soc.* **1996**, *118*, 8891. (b) Kurth, T. L.; Lewis, F. D. *J. Am. Chem. Soc.* **2003**, *125*, 13760. (c) Bryantsev, V. S.; Firman, T. K.; Hay, B. P. *J. Phys. Chem. A* **2005**, *109*, 832.
(33) (a) Weiner, P. K.; Kollman, P. A. *J. Comput. Chem.* **1981**, *2*, 287. (b) Cornell, W. D.; Cieplak, P.; Bayly, C. I.; Gould, I. R.; Merz, K. M., Jr.; Ferguson, D. M.; Spellmeyer, D. C.; Fox, T.; Caldwell, J. W.; Kollman, P. A. *J. Am. Chem. Soc.* **1995**, *117*, 5179.

is insignificantly weighted on the side of the "*trans*" structured molecules, with considerable amounts of other conformers created by the rotation about (O═)C−N bonds. On the basis of their similar thermodynamic stabilities, and prior studies, the low activation barriers for the interconversion of the conformers of **1**−**3** can also be anticipated.

The electrostatic potential maps of **1**−**3**, obtained by semiempirical (AM1) energy minimizations,[34] are shown in Figure 2B. They reveal comparable and slightly electron-deficient aromatic surfaces of **1** and **2.** Compound **3**, however, exhibits a larger negative electrostatic potential at the center of its aromatic core.

Ambiguities in Developing the Predicting Powers. What grants compound **1**, but not **2** and **3**, the ability to gel primary alcohols? The computed conformational behavior of **1**−**3** was shown to be almost identical: all three compounds have many vibrational degrees of freedom and yet show a certain level of preorganization (Figure 2A) enabling them to engage in forming hydrogen bonds and to undergo the longitudinal ordering. The electronic properties of **1**−**3** are, however, distinctive (Figure 2B). According to our findings (Figure 5), the ordering of **1** necessitates $\pi-\pi$ aromatic interactions (Figure 5). This leads to a presumption that the assembly of electron-deficient **1** or **2** would be thermodynamically more favorable than that of more electron-rich **3**. In fact, the electrostatic Hunter/Sanders model,[35] in combination with Siegel and Waters experimental studies,[36] supports the notion of the slipped and stacked π-deficient aromatics as thermodynamically more stable than the corresponding π-rich compounds.

Along with its electron-rich character, the low solubility of **3** in alcoholic solvents (Table S1, Supporting Information) furthermore disqualifies this compound as a gelator. The solubility is likely to result from the absence of the aromatic nitrogen that presumably allows the formation of hydrogen bonds with the alcohols. Actually, the same hydrogen bonding lends **1** and **2** a different solubility behavior (vide supra).

Intriguingly, both **1** and **2** portray almost indistinguishable conformational and electronic properties, and similar solubility behavior. Yet, compound **1** incorporates two additional methyl groups and is structurally different from **2**. On the basis of the X-ray studies of the xerogel of **1** (Figure 5), one of the methyl groups aids the lateral ordering of the columnar assemblies, comprised of stacked and hydrogen bonded aromatics. The role of the methyl is thus prominent in increasing the capacity of the constituent molecules to engage in the hierarchical assembly of **1**, and thereby allowing the effective packing and recognition. Compound **2** has no such capacity, and therefore fails in mediating the gelation. Furthermore, we find that the nature of the surrounding solvent molecules is also critical for the assembly: the gelation was only evidenced for **1** but not **2** suspended in primary alcohols (Table 1). The alcohols are expected to form hydrogen bonds with both **1** and **2**. However, sterically less hindered **2** should have a greater affinity for interacting with the protic solvents. This higher propensity of **2** for binding alcohols increases its solvation energy, which likely obstructs the microphase separation and therefore the solvent gelation. In the case of more substituted and less solvated **1**, the gelation process was not impeded.

Conclusion

The anisotropy of noncovalent interactions is an important and yet insufficient prerequisite for a compound to gel liquids. The structural and electronic properties of small functional molecules, in addition to the solvent characteristics, must be taken into account for a rational design of soft gel materials. Our current understanding of modularly architectured **1**−**3** shows that the electronic and structural features of their aromatic scaffolds, in addition to their propensity to hydrogen bond solvent molecules, all need to be finely balanced to achieve the desired hierarchical assembly and microphase separation. Moreover, the solvent polarity plays an important role in directing the ordering of molecules via the solvophobic effect. This and other solvent parameters necessitate a careful consideration if one is to attempt to engineer a particular morphology in the soft material. The sol−gel phase transition can, interestingly, be promoted with ultrasonication. Presumably, a fast exchange of the assembled aggregates in a supersaturated sol is assisted with sonic waves to allow for the effective and "error-free" organization toward formation of a fully developed 3D network of fibers. The protocol of direct space structure solution of X-ray powder diffraction data, applied here, has been of great assistance in revealing the assembly pattern in the xerogel.[37] It is indeed appealing to use this strategy in the future for directly observing the molecular packing in the intact gel phase.

It is a part of our research program to additionally modify the structure of the aromatics examined herein. The objective is to provide further insight into the mechanism of the gelation, and at the same time allow the preparation of nanostructured soft materials with intriguing properties.

Experimental Section

General Procedure for the Synthesis of Compounds 7−**9.** A solution of **4**−**6** (1.47 mmol) in methanol (80.0 mL) in a 150-mL high-pressure reaction vessel was treated with ammonia gas for approximately 25 min at room temperature. The vessel was capped, and the solution was heated at 55 °C for 3 h. The reaction mixture was left to cool to room temperature for 12 h, and the solvent was evaporated under reduced pressure to yield a solid residue. The solid was dissolved in 20 mL of distilled water and the solution titrated with NaOH (6.0 M in water) until it became basic (pH ∼9). It was then extracted with dichloromethane (3 × 30 mL), and the organic layer was subsequently dried with anhydrous Na_2SO_4, filtered, and evaporated under reduced pressure to yield pure **7**−**9**.

Data for (2,6-dimethylpyridine-3,5-diyl)dimethanamine (7): Yield 84%. ^{1}H NMR ($CDCl_3$) δ 7.54 (s, 1H), 3.85 (s, 4H), 2.49 (s, 6H), 1.4 (br s, 4H); ^{13}C NMR ($CDCl_3$) δ 153.4, 135.2, 133.9, 43.1, 21.6; HRMS (ESI) *m*/*z* calcd for $C_9H_{16}N_3$ 166.1344 $[M + H]^+$, found 166.1347.

Data for pyridine-3,5-diyldimethanamine (8): Yield 56%. ^{1}H NMR ($CDCl_3$) δ 8.46 (d, 1H), 7.67 (t, 2H), 3.92 (s, 4H), 1.42 (br s, 4H); ^{13}C NMR ($CDCl_3$) δ 147.7, 138.2, 134.0, 44.0; HRMS (ESI) *m*/*z* calcd for $C_7H_{11}N_3Na$ 160.0851 $[M + Na]^+$, found 160.0852.

(34) (a) Dewar, M. J. S.; Zoebisch, E. G.; Healy, E. F.; Stewart. J. J. P. *J. Am. Chem. Soc.* **1985**, *107*, 3902. (b) Kamieth, M.; Klärner, F.-G.; Diederich, F. *Angew. Chem., Int. Ed. Engl.* **1998**, *37*, 3303.

(35) (a) Hunter, C. A.; Sanders, J. K. M. *J. Am. Chem. Soc.* **1990**, *112*, 5525. (b) Cockroft, S. L.; Hunter, C. A.; Lawson, K. R.; Perkins, J.; Urch, C. J. *J. Am. Chem. Soc.* **2005**, *127*, 8594.

(36) (a) Cozzi, F.; Siegel, J. S. *Pure Appl. Chem.* **1995**, *67*, 693. (b) Rashkin, M. J.; Waters, M. L. *J. Am. Chem. Soc.* **2002**, *124*, 1860.

(37) (a) Terech, P.; Ostuni, E.; Weiss, R. G. *J. Phys. Chem.* **1996**, *100*, 3759. (b) Ostuni, E.; Kamaras, P.; Weiss, R. *Angew. Chem., Int. Ed. Engl.* **1996**, *35*, 1324. (c) Sakurai, K.; Jeong, Y.; Koumoto, K.; Friggeri, A.; Gronwald, O.; Sakurai, S.; Okamoto, S.; Inoue, K.; Shinkai, S. *Langmuir* **2003**, *19*, 8211.

(38) Reichardt, C. *Chem. Rev.* **1994**, *94*, 2319.

Data for (4,6-dimethyl-1,3-phenylene)dimethanamine (9): Yield 75%. Mp 118−119 °C; ^{1}H NMR ($CDCl_3$) δ 7.24 (s, 1H), 6.97 (s, 1H) 3.83 (s, 4H), 2.29 (s, 6H), 1.42 (br s, 4H); ^{13}C NMR ($CDCl_3$) δ 153.4, 135.2, 133.9, 43.1, 21.6; HRMS (ESI) *m*/*z* calcd for $C_{10}H_{17}N_2$ 165.1391 $[M + H]^+$, found 165.1389.

General Procedure for the Synthesis of Compounds 1−3. To a solution of **7**−**9** (1.31 mmol) in dichloromethane (100 mL), at room temperature and under an atmosphere of argon, was added dropwise neat ethyl isocyanate (2.88 mmol). The solution was left to stir for 12 h, during which a solid precipitate appeared. The solid was filtered, washed with methylene chloride (2 × 10 mL), and dried in air and then under vacuum for 2 h to yield pure **1**−**3**.

Data for compound 1: Yield 66%. Mp 242 °C dec; ^{1}H NMR (CD_3SOCD_3) δ 7.33 (s, 1H), 6.17 (t, 2H, J = 5.8 Hz), 5.81 (t, 2H, J = 5.8 Hz), 4.11 (d, 4H, J = 5.5 Hz), 3.02 (dq, 4H, J_1 = 5.8 Hz, J_2 = 7.0 Hz), 2.37 (s, 6H), 0.99 (t, 6H, J = 7.3 Hz); ^{13}C NMR ($CDCl_3$) δ 157.8, 153.0, 134.9, 130.7, 40.2, 34.1, 21.1, 15.7; HRMS (ESI) *m*/*z* calcd for $C_{15}H_{25}N_5O_2Na$ 330.1906 $[M + Na]^+$, found 330.1902.

Data for compound 2: Yield 64%. Mp 210 °C; ^{1}H NMR ($CDCl_3$) δ 8.31 (d, 2H, J = 2.0 Hz), 7.49 (t, 1H), 6.35 (t, 2H, J = 5.8 Hz), 5.90 (t, 2H, J = 6.2 Hz), 4.19 (d, 4H, J = 6.0 Hz), 3.02 (dq, 4H, J_1 = 5.6 Hz, J_2 = 7.0 Hz), 0.99 (t, 6H, J = 7.1 Hz); ^{13}C NMR ($CDCl_3$) δ 157.9, 146.9, 136.0, 133.6, 40.5, 34.2, 15.6; HRMS (ESI) *m*/*z* calcd for $C_{13}H_{21}N_5O_2Na$ 302.1593 $[M + Na]^+$, found 302.1592.

Data for compound 3: Yield 54%. Mp 215 °C dec; ^{1}H NMR ($CDCl_3$) δ 8.31 (s, 1H) 7.49 (s, 1H), 6.01 (t, 2H), 5.75 (t, 2H), 4.11 (d, 4H, J = 5.6 Hz), 3.02 (dq, 4H, J_1 = 6.0 Hz, J_2 = 7.2 Hz), 2.19 (s, 6H), 0.98 (t, 6H, J = 7.2 Hz); ^{13}C NMR ($CDCl_3$) δ 157.8, 135.4, 133.9, 131.7, 127.8, 41.0, 34.1, 18.0, 15.7; HRMS (ESI) *m*/*z* calcd for $C_{16}H_{26}N_4O_2Na$ 329.1953 $[M + Na]^+$, found 329.1952.

General Procedure for the Preparation of Gels. Compound **1** was placed in a glass vial, and 0.5 mL of solvent was added. The vial was capped, and the cap was pierced with a needle. The solution was heated with a heat gun until the solid completely dissolved, after which it was sonicated in an ultrasound bath to allow for the gel formation.

IR Experiments. IR spectrophotometers, used in the study, were equipped with a DTGS KBr detector. FT-IR spectra of 32 scans were obtained with 4 cm^{-1} resolution. A demountable IR cell equipped with an attenuated total reflectance ZnSe window was utilized for obtaining the ATR spectra (Figure 4A/B). A long path, 10 mm, liquid cell with KBr windows was used for obtaining the spectrum shown in Figure 4C.

X-ray Powder Diffraction and Simulated Annealing. The X-ray powder diffraction spectrum of **1** was collected in Bragg−Brentano geometry on a diffractometer (40 kV, 50 mA, Cu $K\alpha_1$ radiation) equipped with a Ge 111 incident beam monochromator and a linear position sensitive detector. The data were taken from 3 to 50° 2θ with a step size of 0.007168° 2θ and a dwell time of 3 s.

Transmission Electron Microscopy. TEM measurements were conducted with a CM 12 Transmission Electron Microscope (STEM). A small quantity of gel was placed onto a carbon-coated TEM grid to form a thin layer. The solvent was removed under vacuum, and the sample was placed directly into the microscope without negative staining. Images were recorded at selected areas of the grid, at magnifications ranging from ×6800 to ×150000.

Molecular Modeling. Molecular modeling (Figure 2A) was carried out by molecular mechanics calculations. The calculations were performed by employing the Amber force field as implemented in the Maestro software. A Monte Carlo conformational search (torsional sampling 100 000 steps, energy window for saving structures 20 kJ/mol) generated conformers whose distribution population was analyzed by the Boltzmann equation. The global minimum conformers (**1**$_a$−**3**$_a$, Figure 2A) were further optimized by using the semiempirical AM1 method to generate the corresponding electrostatic potential maps.

Acknowledgment. We thank Professor Christopher M. Hadad of the Ohio State University and Dr. Sasha Stankovich of Northwestern University for useful suggestions. This work was financially supported with funds obtained from the Ohio State University.

Supporting Information Available: Additional experimental results and spectra for all new compounds. This material is available free of charge via the Internet at http://pubs.acs.org.

JO071159Y